ISSN 1019-3316, Herald of the Russian Academy of Sciences, 2016, Vol. 86, No. 6, pp. 426–432. © Pleiades Publishing, Ltd., 2016.
Published in Russian in Vestnik Rossiiskoi Akademii Nauk, 2016, Vol. 86, No. 12, pp. 1073–1080.

Reports by the Laureates of the 2015 Lomonosov Grand Gold Medal of the Russian Academy of Sciences

Probing Quantum Systems from the Inside While Producing the World's Shortest Optical Pulses[1]

Paul Corkum[1]*

Joint Attosecond Science Laboratory, University of Ottawa and the National Research Council of Canada, Room 464, Advanced Research Complex, Ottawa, ON, Canada K1N 6N5

[1]*e-mail: pcorkum@uottawa.ca*

Received June 27, 2016

Abstract—In 1964, Professor L.V. Keldysh, with whom I share winning the Lomonosov Gold Medal, published what was to become a very influential paper. In his paper, he developed the theory of multiphoton ionization for atoms and the creation of electron-hole pairs for solids. Fifty years later, we generate the world's shortest light pulses using electron wave packets that are extracted from rare gas atoms by an intense infrared pulse much as Professor Keldysh described. The ultrashort bursts of XUV radiation from many atoms add coherently to produce intense pulses as short as 65 attoseconds—the current world record. Similar highly nonlinear processes occur in other atoms, molecules and solids. In addition to its importance as a new source of soft X-ray radiation and ultrashort pulses, the radiation generated from ionizing material encodes information on the quantum system from which it was made. By analyzing the XUV radiation, not only can we image molecular orbitals but also determine the band structure of solids.

Keywords: tunneling, multiphoton ionization, attosecondpulses,re-collisions, electronwavepacket.

DOI: 10.1134/S1019331616060125

It is a great honor to share the Russian Academy of Science's Lomonosov Gold Medal with Professor Keldysh. His research has inspired a generation of researchers, including me and many of the students in my group even today.

This paper covers the material that I described in my acceptance lecture on March 22, 2016. Therefore, it is not meant as a comprehensive review of the field, but rather a personal perspective. You will see how my research builds on the work of Professor Keldysh. I specifically refer to his work on photo-ionization in gases and his research on valence-to-conduction band transitions in solids [1] which has had an important influence on plasma physics, atomic physics, optical physics and solid state physics.

I entered the field of multiphoton ionization from plasma physics in the late 1980s. When an atomic gas absorbs photons, it is transformed into a plasma. The newly formed plasma will, in general, be far from equilibrium and the disequilibrium will depend critically on the colors and polarization of the light. Plasmas with the resulting characteristics [2, 3] would be impossible to form otherwise. The disequilibrium arises because (1) the ion kinetic energy is almost unaffected by ionization and can be very cold; (2) the ionization energy consists of population in a range of excited states; and (3) the free-electrons gain energy during ionization in a process known as "Above-Threshold-Ionization" (or ATI). In an isolated atom this energy gain comes mainly from the electron's interaction with the laser field. In a plasma, all electric fields (both laser and plasma fields) contribute to the energy gain. These highly non-equilibrium plasmas provide routes to producing ultracold plasmas [4], X-ray lasers [5] and even lasers in the air [6, 7].

In this paper, I will concentrate on the same problem from an atomic perspective. When an atom (or molecule) ionizes, an electron wave packet is produced in the continuum. The total wave function of the ionizing electron has two important components: the ground state in which some of the initial electron wave function resides, and the wave packet. In the multiphoton case (especially under tunneling conditions) once created, the electron wave packet undergoes oscillatory motion in the intense light required to ionize the atom. This oscillatory velocity can easily exceed the drift velocity: if that happens, portions of the electron wave packet can return to the ion from which it originated. This is called re-collision [3]. Through re-collision, multiphoton ionization opens new ways to probe

[1] The article was translated by the author.

* Paul Corkum is a Professor in the Department of Physics, University of Ottawa and Head of the attosecond pulses research program at the National Research Council of Canada.

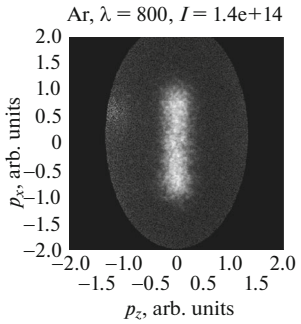

Fig. 1. A 2-dimensional projection of the momentum distribution of electrons ionized from argon atoms by a circularly polarized, 50 femtosecond, 800 nm pulse with peak intensity of 2×10^{14} W/cm^2. The light is propagating along the z-direction. The momentum distribution in the z direction shows the natural spread of the electron wave packet that is determined by tunneling. The figure is reproduced from [14].

matter [8, 9], new ways to produce soft X-ray radiation [10] and new ways to make short pulses [11, 12].

So we shall start with the basics—tunneling.

Tunneling. Professor Keldysh provided us with a means to determine realistic intensities in multiphoton ionization experiments and therefore, to estimate the importance of re-collision. He showed that when a sufficiently intense, infrared light pulse irradiates atoms two limiting cases result: Their boundary is marked by a parameter that has since become known as the Keldysh parameter

$$\gamma = \left(\frac{IP}{2U_p}\right)^{1/2},$$

where IP is the ionization potential of the atom in question and $U_p = \frac{q^2E^2}{4m\omega^2}$. Here, q and m are the electronic charge and mass, respectively, E is the peak laser field (assuming linearly polarized light), and ω is the angular frequency of the light. In one case, $\gamma < 1$,—ionization can be approximated by tunneling. Specifically, the ionization probability can be approximated by the DC tunneling formula at any instant of time. For 800 nm light and an ionization potential of 15 eV, the $\gamma = 1$ boundary occurs at an intensity of about 1.3×10^{14} W/cm^2. In the other case, $\gamma > 1$, ionization is perturbative.

We can estimate the intensity required for a hydrogen atom to tunnel-ionize in a 10 femtosecond pulse. Let us assume that we wish to ionize with 10% ionization probability—that is, we wish an ionization rate of 10^{13} s^{-1}. The equation for tunneling is:

$$\omega(t) = \omega_0 \frac{E_a}{E(t)} \exp\left[-\frac{2}{3}\frac{E_a}{E(t)}\right],$$

where ω_0 is the atomic frequency. E_a is the atomic field, and $E(t)$ is the magnitude of the light field at time, t. Substituting $\omega(t) = 10^{13}$ s^{-1} we obtain $E(t) = 3 \times 10^8$ V/cm or $I \sim 10^{14}$ W/cm^2. This result is near, although slightly lower than, the experimental intensity required to ionize argon, an atom with a similar ionization potential, with a femtosecond pulse. Therefore, we can use tunneling to approximate ionization in many experiments that use 800 nm light.

Tunneling equations predict that, because we require such a high ionization rate for femtosecond experiments, an electron will have a significant probability of tunneling to excited states. While the reason is not obvious in the equation above, it arises because the exponential term is relatively large (here about 10^{-6}). Therefore, in experiments that use short pulses we produce molecules in both the ground state and in an excited state. This provides the basic population in the excited state for lasing in the N_2^+ ion in air [6].

The electron wave packet as it emerges from the tunnel. It is important to ask, "what are the characteristics of the electron wave packet that tunneling produces." In the laser field direction the wave packet motion is dominated by the time-dependent field of the light wave and, as we will see below, the electron is prone to re-collide with its parent ion if it moves in linear polarized light. However, with *circular polarized light and in the propagation direction of the light beam*, the electron does not gain added momentum from the field (except the small photon momentum) [13]. Therefore, if we measure the momentum distribution of the ionizing electron in this direction, we observe the nascent electron's momentum acquired during the elementary process of tunneling.

Figure 1 is obtained using a velocity-map-imaging electron spectrometer. (Velocity map imaging refers to an electron lens array that maps two dimensions of the electron velocity distribution onto two spatial dimensions on a detector. In other words, the image on the screen is an image of a two-dimensional projection of the electron wave packet's momentum wavefunction.) Figure 1, taken from [14], shows a velocity map image of circular polarized light interacting with argon atoms. In the figure, the light is propagating along the axis labeled P_z. The Gaussian distribution of momenta maximizes near zero and extends to a fraction of an atomic unit. This distribution arises from a convolution of the characteristic transmission probability of the tunnel convolved with the bound-state electron wavefunction from which the electron tunneled.

We can test if the emerging electron retains some information on the bound state orbital from which it departed by making a similar measurement on a more complex orbital and by using a molecule so the orbital projection can be experimentally controlled. In Fig. 2, taken from [15], we show the normalized difference of the momentum distribution of the electron that has emerged from an oxygen (left) or a nitrogen (right)

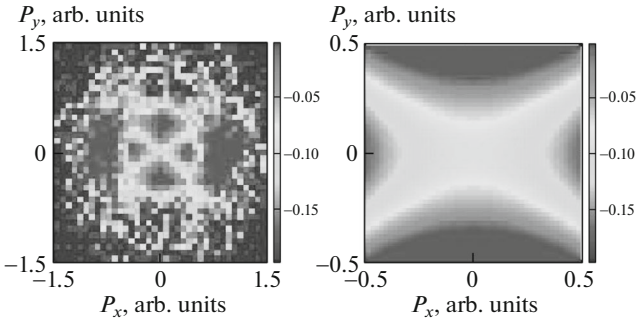

Fig. 2. A two dimensional projection of the normalized difference of the momentum distributions between electron wave packets extracted from O_2 (left) and N_2 (right). The 800 nm ionizing beam was a linearly polarized along the z-direction with peak intensity of 2×10^{14} W/cm^2. The electric field direction is perpendicular to the figure's plane. The normalized difference is for the molecule aligned perpendicular to the light polarization—the molecule randomly aligned. The figure is reproduced from [15].

molecule. In both cases, the normalized difference was obtained for linearly polarized light and the difference is between the distributions obtained when the molecule is aligned perpendicular to the laser field direction, minus when the molecule is randomly aligned. While the symmetry of the oxygen orbital is strikingly revealed in the figure, the image is distorted by re-collision, which we will deal with next.

Semi-classical motion in the strong field. Electron motion in the direction of the light field is most easily understood classically. (That classical physics even approximates an atomic problem may seem surprising. However, in re-collision physics, we are usually concerned with processes involving 10s, 100s, 1000s (or even more) photons, and in this high-photon-number limit, multiphoton effects can often be understood classically.)

Figure 3 illustrates the basic classical motion of the electron. The atom in the illustration shows a classical electron emerging over the Coulomb barrier just following a crest in the light field. Once the electron has passed through the tunnel, the strongest influence on its motion is the electric field of the light wave (illustrated by the sinuous smooth line). Therefore, the electron leaves the region of the ion core. Depending on the moment of birth, the electron is forced to re-collide at a time and energy that can be determined using classical equations of motion. In other words, classically a moment-of-birth is mapped into an energy and time-of-collision by $F = ma$.

Classical physics predicts that the maximum re-collision energy of the electron is given by $3.17U_p$. This basic scaling shows that more energetic electrons are found for higher ionization potential atoms because they can reach higher intensities before they ionize. The basic scaling also motivates the current research drive to use intense mid-infrared pulses for ionizing atoms, thereby reaching higher re-collision energies (and therefore high harmonics in the X-ray region). The current state-of-the-art uses 3 micron photons to ionize helium, which produces soft X-ray radiation with photon energy in excess of 1 keV [10].

Approximately this same $3U_p$ value that we find classically also shows up in all quantum calculations, including solutions of the time-dependent Schrodinger equation, where it was initially found that the highest harmonic produced in a simulation had photon energy up to $IP + 3U_p$ [16].

A semi-classical approximation to quantum mechanical motion allows us to interpret classical trajectories as quantum trajectories. Semi-classically, components of the tunneling electron wave packet follow classical-like trajectories, accumulating phase along the way and re-colliding with a time and energy that is approximately predicted by classical physics.

The re-collision electron is not only a source of high harmonic radiation (which we will discuss next). It is also a projectile extracted from a quantum system

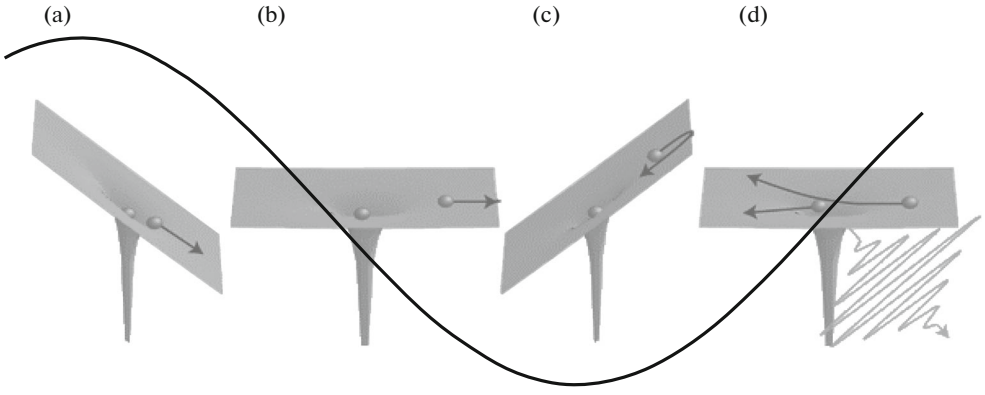

Fig. 3. A qualitative figure illustrating one classical trajectory of the many that contribute to high harmonic generation. In frame (a) the electron emerges from the atom under the influence of the intense ionizing field, shown by the sinuous smooth line. In frames (b and c) the electron moves under the influence of the light field. Frame (d) captures the electron as it re-collides. It can scatter from its parent ion or it can recombine, emitting light.

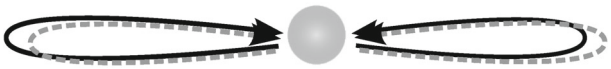

Fig. 4. An illustration of high harmonic generation wherein we follow two trajectories (dashed lines) that are identical except they are delayed by 1/2 period from each other. A weak second harmonic field can add action to one trajectory and subtract action from the other. This breaks symmetry and leads to even harmonic emission. Each trajectory has an optimum phase difference between the fundamental and its second harmonic to maximally break symmetry.

and is sent back where it can probe its former self. For example, the electron can diffract, revealing the molecule's structure in the diffraction pattern [8, 15], or it can recombine, emitting radiation through the oscillating dipole moment. In the approximation where the re-colliding electron can be taken as a plane wave, the dipole moment is a Fourier transform that contains sufficient information to reveal orbital wave function. Thus the electron probes the wavefunction structure of the ground state from which it left and to which it returns. This is the most extreme case of the electron molecule probing itself from the inside [9].

Attosecond pulses and high harmonics. From Fig. 3 we see that an electron wave packet born near one field crest returns following the next field crest, emitting radiation as suggested by classical physics. Confining the process of ionization and re-collision to just one re-collision produces an attosecond pulse. Various technologies have been developed to ensure that this can be engineered. Since the pulses are naturally chirped (as you will see from a classical calculation), reaching a 65 attosecond pulse duration requires chirp compensation. This can be achieved with metal filters that can be selected to remove the nascent chirp on the pulse. The limited range of chirp compensation available from filters currently sets the limit on the achievable pulse duration.

In contrast, if the process is repeated over a few half cycles, we create a train of attosecond pulses. As illustrated in Fig. 4, semi-classical physics encourages us to think of the underlying process of high harmonic generation in terms of an electron interferometer. As we know from optics, an interferometer is a very valuable instrument. With an interferometer, we are usually concerned with adjusting the relative phase of the light in each arm. The phase of the electron in our electron interferometer can be adjusted by combining a weak second harmonic field with the fundamental. As the relative phase of the two beams is changed, action is added to (or subtracted from) one side of the interferometer or the other.

It is important to consider at what relative phase between the fundamental and second harmonic we optimally unbalance each quantum trajectory. Remembering the mapping between trajectory and photon energy, this is equivalent to asking "what is the phase that optimally creates any frequency of even harmonics"? It is conceptually clear and experimentally confirmed [17] that this frequency-dependent phase difference (or spectral phase) is characteristic of the re-collision process, and allows us to measure the chirp on the re-collision electron that will produce the attosecond pulse.

Before turning to solids, it is important to note that re-collision is not the only source of harmonics from an ionizing gas [18]. Ionization in the tunneling limit occurs in a step-wise manner and this gives step like behaviour to the resulting electron current

$$J(t) = qn_e(t)v(t).$$

Here, q is the electronic charge, $n_e(t)$ is the number of free electrons as a function of time, and $v(t)$ is the velocity of the free electrons. The step-wise nature of this current provides a non-re-collision source in Maxwell's equations. This step-wise source contributes to the relatively lower harmonics. With that, we turn to wide bandgap semiconductors where Professor Keldysh's ideas might lead us to expect similar physics.

Wide bandgap semiconductors. While studies of the interaction of intense light with gases has led to (1) a new source of soft X-rays, (2) light pulses with duration of less than 1 femtosecond, and (3) a new way to probe materials, studies in solids have mostly concentrated on laser machining. These two solitudes had minimum influence on each other. Of course, they shared multiphoton ionization, which offered some potential for unique diagnostics [19–21]. However, until recently there has not been much work on the extreme nonlinear optical response of solids. This is now changing rapidly.

The primary cause of this change is the discovery that high harmonics of mid-infrared (~3.5 μm) light can be generated in ZnO (a wide band gap semiconductor [22]) and in SiO_2, a dielectric [23]. Here we concentrate on ZnO. To begin the transition to semiconductors, it is helpful to re-express atomic re-collision in band structure language.

In atomic gases, multiphoton ionization in the tunneling limit creates both an electron and ion each having approximately zero momentum. Tunneling can be represented by the small red arrow on Fig. 5. The electron and ion both move on their respective bands, gaining equal momentum from the field (as we know from conservation of momentum). The electron band structure is parabolic, while the band for the heavy ion is approximately a horizontal line.

Re-collision means that the electron and ion find each other in physical space, where the electron recombines with the ion, emitting a photon (shown as the blue arrow in Fig. 5). In solid-state language, they make a band-to-band transition at the momentum that the electron and hole possess when they re-collide. This suggests that it would be important to

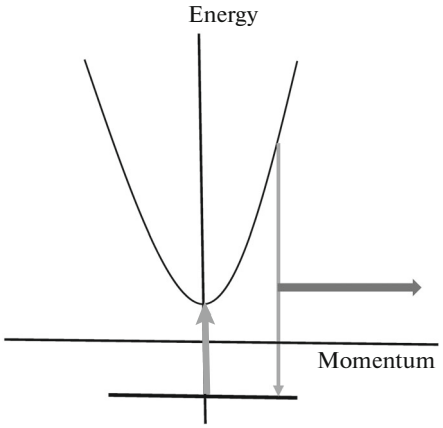

Fig. 5. A solid state-like presentation of the gas phase high harmonic process. Tunneling transfers an electron to the continuum, creating thereby an electron moving on a parabolic band and an ion, moving on a band that is essentially flat. As the electron and ion both move in momentum space they find each other in physical space and make a vertical transition to recombine.

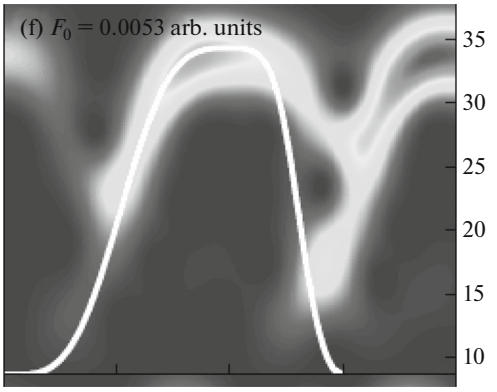

Fig. 6. The figure, calculated for ZnO irradiated with 3.5 micron light, shows the photon energy plotted on the vertical axis as a function of the time (or phase) within a period of the driving laser field. The color code shows the light intensity and the white line is the result of a semiclassical calculation if electron hole motion using band-corrected masses. The figure is taken from [24].

develop a two-band model of harmonic generation from solids.

Using a band structure as close as possible to that of ZnO, a two-band model allows the parallel between solid and gas phase experiments [24, 25] to be explored. High harmonics are predicted by the model, but what is their origin?

Figure 6 plots the results of a gated Fourier transform that shows the time (horizontal axis) when a given frequency of the emission (vertical axis) is emitted within a single cycle of the fundamental field. We see that the signal begins with low frequency and then sweeps to high frequency as the cycle progresses. This is qualitatively similar to what we measure for gases and what we predict from the trajectories we calculate with $F = ma$. In fact, the white line on the figure is obtained by a classical calculation in which the electron moves with band-corrected masses. Thus, the two-level model suggests that the dominant mechanism of harmonic generation in ZnO is re-collision.

It is important to confirm this interpretation experimentally [26]. To do so, we turn to the two-color measurement described previously and illustrated in Fig. 4. (Recall, the idea is that a weak second harmonic modifies the electron trajectory between ionization and re-collision.) If a single-frequency multicycle driver is used, we should observe only odd harmonics from a symmetric system. The addition of even a weak second harmonic breaks the symmetry and the optimum symmetry breaking identifies the trajectory.

Figure 7 is a map that shows the harmonic number plotted along the horizontal axis and the relative phase between a fundamental and its second harmonic plotted along the vertical axis. For this measurement we used a 3.5 μm fundamental beam with peak intensity of 10^{12} W/cm^2 and a second harmonic intensity of 10^7 W/cm^2. The figure shows that the odd harmonics signal is much stronger than the even harmonics. The pink line joins the minima in the even harmonic signal for subsequent even harmonics. This relative delay is evidence of the varying spectral phase (or time-of-emission) of the associated frequency component. This varying spectral phase is characteristic of re-collision. It shows that re-collision is the source of the high harmonics from ZnO.

Concluding comments. It remains unclear how general the re-collision nature of the harmonics might be for solids. In my lab, we find similar re-collision-like behavior for silicon [27], but it seems unlikely that the source or harmonics in SiO_2 will be the same [23]. Still, for an important class of materials, the connection between gases and solids has been made. There are a number of general implications. By way of conclusion, we mention just a few.

1. Solids can become a home for some aspects of attosecond technology. Shedding the need for high vacuum systems greatly simplifies attosecond technology and increases its impact.

2. With the sensitivity to perturbing fields that we have recorded with our *in-situ* measurement in ZnO, and the observation of high harmonics from silicon, a route is opened to integrate extreme nonlinear optics with modern electronics. Extreme nonlinear optics can provide three advantages (1) time resolution sufficient to observe any electronic response in any circuit, (2) spatial resolution of the shortest wavelength light generated internally in the material, and (3) field sensitivity (through symmetry-breaking) on the scale of those in conventional electronic circuits.

3. Re-collision physics allows a system to "probe itself." This is true for laser-induces-electron-diffrac-

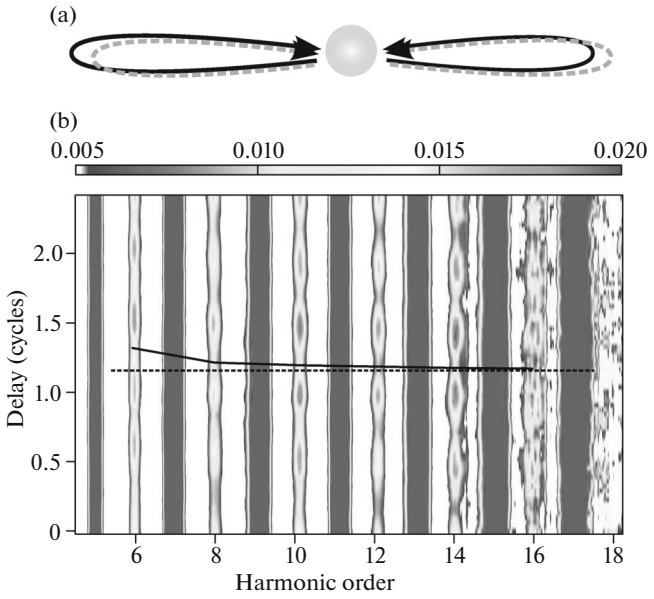

Fig. 7. (a) Reproduction of Fig. 4, illustrating the point of the measurement. (b) Experimental map where the measured harmonic order is plotted on the horizontal axis and the relative phase between the fundamental pulse ($I = 10^{12}$ W/cm^2) and its second harmonic ($I = 10^7$ W/cm^2) is on the vertical axis. The pink curve shows the relative phase for each harmonic where the symmetry is optimally broken. The harmonic order dependence of the optimum phase agrees with that predicted by the two band model. It is consistent with a re-collision origin for the harmonic emission in ZnO. The figure is taken from [24].

tion [8], orbital tomography [9], and perhaps for electronic circuits. It may also be possible to use self-probing to watch rapid band collapse in laser irradiated materials or to measure the band structure of materials under ultra-high pressure [28].

In conclusion, I am honored to share the Lomonosov Gold Medal with Professor Keldysh. It has been just over 50 years since Professor Keldysh's initial paper. I think that you will agree that the subject that he introduced is still fresh.

ACKNOWLEDGMENTS

I am pleased to acknowledge Canadian financial support from the National Research Council of Canada, Natural Science and Engineering Research Council, Canada Foundation for Innovation, and the Ontario Research Fund. Financial support from US agencies has also been critical and I gratefully acknowledged their contribution. It includes a grant from the US AFOSR (FA9550-13-1-0010), the US ARO (W911NF-14-1-0383) and the DARPA PULSE program through a grant from AMRDEC (W31P4Q1310017). I have also benefited from many helpful discussions with all of my colleagues and students in the Joint Attosecond Science Laboratory at both the National Research Council of Canada and the University of Ottawa. Without their help and support, this work would not have been possible.

REFERENCES

1. L. V. Keldysh, "Ionization in the field of a strong electromagnetic wave," Zh. Eksp. Teor. Fiz. **20**, 1307–1314 (1965).
2. P. B. Corkum, N. H. Burnett, and F. Brunel, "Above threshold ionization in the long wavelength limit," Phys. Rev. Lett. **62**, 1259–1262 (1989).
3. P. B. Corkum, "A plasma perspective on strong field multiphoton ionization," Phys. Rev. Lett. **71** (13), 1994–1997 (1993).
4. J. P. Morrison, C. J. Rennick, J. S. Keller, and E. R. Grant, "Evolution from a molecular Rydberg gas to an ultracold plasma in a seeded supersonic expansion of NO," Phys. Rev. Lett. **101**, 205005 (2008).
5. N. H. Burnett and P. B. Corkum, "Cold plasma production for recombination XUV lasers by optical field induced ionization," J. Opt. Soc. Am. B **6**, 1195–1199 (1989).
6. Y. Liu, Y. Brelet, G. Point, A. Houard, and A. Mysyrowicz, "Self-seeded lasing in ionized air pumped by 800 nm femtosecond laser pulses," Optics Express **21**, 22791–22798 (2013).
7. H. Zhang, C. Jing, J. Yao, et al., "Rotational coherence encoded in an 'air-laser' spectrum of nitrogen molecular ions in an intense laser field," Phys. Rev. X **3**, 041009 (2013).
8. T. Zuo, A. D. Bandrauk, and P. B. Corkum, "Laser induced electron diffraction: A new tool for probing ultrafast molecular dynamics," Chem. Phys. Lett. **259**, 313–320 (1996).
9. J. Itatani, J. Levesque, D. Zeidler, et al., "Tomographic imaging of molecular orbitals," Nature **432**, 867–871 (2004).
10. T. Popmintchev, M.-C. Chen, D. Popmintchev, et al., "Bright coherent ultrahigh harmonics in the keV X-ray regime from mid-infrared femtosecond lasers," Science **336**, 1287–1291 (2012).
11. P. B. Corkum, N. H. Burnett, and M. Y. Ivanov, "Subfemtosecond pulses," Opt. Lett. **19** (22), 1870–1872 (1994).
12. M. Hentschel, R. Kienberger, C. Spielmann, et al., "Attosecond metrology," Nature **414**, 509–513 (2001).
13. C. Smeenk, L. Arissian, B. Zhou, et al., "Partitioning of the linear photon momentum in multiphoton ionization," Phys. Rev. Lett. **106**, 193002 (2011).
14. L. Arissian, C. Smeenk, F. Turner, et al., "Direct test of laser tunneling with electron momentum imaging," Phys. Rev. Lett. **105**, 133002 (2010).
15. M. Meckel, D. Comtois, D. Zeidler, et al., "Laser induced electron tunneling and diffraction," Science **320**, 1478–1482 (2008).
16. J. L. Kraus, K. J. Schafer, and K. C. Kulander, "High-order harmonic generation from atoms and ions in the high intensity regime," Phys. Rev. Lett. **68**, 3535–3558 (1992).

17. N. Dudovich, O. Smirnova, J. Levesque, et al., "Measuring and controlling the birth of attosecond XUV pulses," Nature Physics **2**, 781–786 (2006).
18. F. Brunel, "Harmonic generation due to plasma effects in a gas undergoing multiphoton ionization in the high-intensity limit," J. Opt. Soc. Am. **7**, 521–526 (1990).
19. M. Gertsvolf, H. Jean-Ruel, P. P. Rajeev, et al., "Orientation-dependent multiphoton ionization in wide band gap crystals," Phys. Rev. Lett. **101**, 243001 (2008).
20. D. Grojo, M. Gertsvolf, S. Lei, et al., "Exciton-seeded multiphoton ionization in bulk SiO_2," Phys. Rev. B **81**, 212301 (2010).
21. M. Gertsvolf, M. Spanner, D. M. Rayner, and P. B. Corkum, "Demonstration of attosecond ionization dynamics inside transparent solids," J. Phys. B **43**, 131002 (2010).
22. S. Ghimire, A. D. DiChiara, E. Sistrunk, et al., "Observation of high-order harmonic generation in a bulk crystal," Nature Physics **7**, 138–141 (2011).
23. T. T. Luu, "Extreme ultraviolet high harmonic spectroscopy of solids," Nature **521**, 498–502 (2015).
24. G. Vampa, C. R. McDonald, G. Orlando, et al., "Theoretical analysis of high-harmonic generation in solids," Phys. Rev. Lett. **113**, 073901 (2014).
25. G. Vampa, C. R. McDonald, G. Orlando, et al., "Semiclassical analysis of high harmonic generation in bulk crystals," Phys. Rev. B **91**, 064302 (2015).
26. G. Vampa, T. J. Hammond, N. Thiré, et al., "Linking high harmonics from gases and solids," Nature **522**, 462–464 (2015).
27. G. Vampa, T. J. Hammond, N. Thiré, et al., "Generation of high harmonics from silicon", Preprint No. arXiv:1605.06345arXiv (2016).
28. G. Vampa, T. J. Hammond, N. Thiré, et al., "All-optical reconstruction of crystal band structure," Phys. Rev. Lett. **115**, 193603 (2015).